

MECHANICAL, CHEMICAL, METALLURGICAL CHARACTERISTICS UNDER HBSS SOLUTION AND OPTIMIZATION OF AZ91D - Ti FUNCTIONAL GRADED COMPOSITES USING TOPSIS

S. Tharaknath¹ and I. Rahamathullah²

¹Department of Mechanical Engineering, Podhigai College of Engineering and Technology, Tirupattur, Tamilnadu, India

²Department of Mechanical Engineering, Government College of Engineering, Srirangam, Trichy, Tamilnadu, India

(Received June 29, 2022; Revised August 5, 2022; Accepted August 12, 2022)

ABSTRACT. Functional graded magnesium matrix composites (FGMMCs) are widely employed for biomedical, aerospace and thermal barrier applications because of their better mechanical properties, biocompatibility and bioactivity. In this study, AZ91D-wt. %Ti (x = 0, 4, 8, 12 and 16) composites are fabricated by ex-situ centrifugal casting method. The NaCl based solution is sprayed on all fabricated magnesium composites for 72 hours at the 1 kg/cm³ pressure spray and 6.9 pH value in salt spray chamber. The microhardness and flexural strength of fabricated composites are determined. The corrosion resistance of AZ91D-wt. %Ti fabricated composites is determined for 21 days immersion. The AZ91D -12wt. %Ti exhibits higher microhardness, flexural strength and corrosion resistance than other produced AZ91D-Ti composites. The optimization on micro machining process parameters is done on the AZ91D-12wt. %Ti with the help of Technique for order of preference by similarity to ideal solution (TOPSIS). The input process parameters are selected as cutting rate, feed rate, depth of cut and tool type and the response parameters are selected as feed force, normal force, tool wear rate, burr height and surface roughness. The computed optimal micro milling process parameters are at 120 m/min cutting speed, 0.5 μm feed rate, 0.15 mm depth of cut and the TiB₂ coated tool.

KEY WORDS: AZ91D -Ti, TOPSIS, Surface roughness, Tool wear loss, Cutting force

INTRODUCTION

FGMMCs are combination of two or more distinct materials mixed together to obtain required properties [1]. Metals, polymers, ceramics and their composites are currently used as biomaterials because of their good biocompatibility and bioactivity [2]. Magnesium and its alloys can reduce the stress shielding by their low modulus property. The modulus of Mg and its alloys closes to bone modulus [3]. Titanium (Ti) has better biocompatibility and bioactivity property and it can be used for biomedical applications. Titanium has better corrosion resistance in human body [4]. The bioactivity and biocompatibility of AZ91D - HA composite is in the need of enhancement because it has low corrosion and mechanical property while compare to other AZ91D based composites [5]. Functional graded materials (FGMs) are mostly fabricated by solidification processing methods. The solidification processing methods is very suitable for producing large size components in low cost. Centrifugal casting is widely used for producing FGM materials among various solidification processing methods because it is a simplest and cost effective technique [6, 7]. Biodegradable material should have good mechanical property, corrosion resistance and adequate degradation rate in human body [8]. Micro machining has inconsistent in finding tool wear, formation of burr, chatter and tool setting errors and these draw backs should be rectified [9-11]. The prediction of all kind of responses in connection with all kind of input parameters is accurately predicted by optimization techniques [11-12]. The addition of boron carbide increases the hardness and ultimate tensile strength of the AZ91D matrix material [13].

*Corresponding author. E-mail: tharaknath.research@gmail.com

This work is licensed under the Creative Commons Attribution 4.0 International License

The increasing particle size of silicon carbide decreases the mechanical properties of AZ91D matrix material [14]. The addition of titanium carbide increases the corrosion resistance of AZ91D matrix material [15]. Therefore, no investigation has been made on the fabricating and optimizing the micro machining parameters of AZ91D – Ti composites to satisfy the biocompatibility and bioactivity requirements for biomedical applications. So in this research, AZ91D and Ti have been chosen as matrix material and reinforcement materials respectively to fabricate the AZ91D-wt.%Ti ($x = 0, 4, 8, 12$ and 16) composites with the help of ex-situ centrifugal casting. The better combination of AZ91D – Ti composites has been identified by comparing microhardness, flexural strength and corrosion resistance properties. The optimization of micro milling process parameters is done on the fabricated AZ91D-12wt.%Ti composites with the help of TOPSIS.

EXPERIMENTAL

Materials

The corrosion, biocompatible and other mechanical properties of AZ91D and Ti materials are high. The AZ91D magnesium alloy was chosen as matrix material because of its low modulus and reducing stress shielding properties and titanium was chosen as reinforcement material because of its high corrosion resistance property to form the AZ91D-wt.% Ti ($x = 0, 4, 8, 12$ and 16) composites [16]. The purity of titanium and magnesium was 99 and 99.5%, respectively. The AZ91D magnesium alloy was used in round rod form and titanium was used in powder form. The particle size of titanium powder was measured by using particle size analyzer (PSA) [17]. The titanium powder has an average particle size of 40 μm .

Fabrication of composites

The high specific strength, flexural strength, microhardness and corrosion resistant properties are very important for biomedical, aerospace and thermal barrier applications. The AZ91D-Ti composites has better properties than aluminum based composites because of the presence of magnesium and titanium. The weight percentage of titanium in AZ91D based composites was selected based on the literature. The addition of titanium increases the corrosion resistance of AZ91D based composites. The titanium has the ability to resist corrosion. The AZ91D-wt.%Ti ($x = 0, 4, 8, 12$ and 16) composites were fabricated by using ex-situ centrifugal casting [18, 19]. The AZ91D magnesium alloy was cut into small pieces and placed into crucible of stir casting setup. The many trials were done for choosing melt temperature, speed and duration of stirring for casting the composites and better parameters were selected for stir casting. The AZ91D magnesium alloy was started to melt at 950 °C. The titanium powder was preheated at 1100 °C for 15 min. The preheated titanium powder was stirred in melted magnesium alloy AZ91D at the speed of 300 rpm and duration for 10 min. The centrifugal casting mould was preheated at 250 °C for 15 min. The centrifugal casting mould was rotated at 1500 rpm for duration of 45 s. The melted molten AZ91D-Ti composite was poured in the rotating centrifugal mould. The procedure was repeated for producing AZ91D-Ti ($x = 0, 4, 8, 12$ and 16) composites. This work piece was cut and unrolled by heating for flattening in such a way that the mechanical properties remain unaffected and physical properties were intact as well. The cylindrical form was converted into flat form without affecting the properties of the composites. The tubular samples were unrolled to flat rectangular pieces that do 100 mm long and 50 mm wide possess a thickness of 6 mm.

Testing of composites

EDAX testing

The fabricated specimen was subjected to energy dispersive X-ray analysis (EDAX) for identifying the weight percentage of AZ91D matrix material and titanium reinforcement in AZ91D-Ti composites. The EDAX test is conducted with the help of HITACHI MODEL S-3000 EDAX tester.

Mechanical, chemical and metallurgical property testing

The NaCl based solution is sprayed on all fabricated magnesium composites for 72 hours at the 1 kg/cm³ pressure spray and 6.9 PH value in spray chamber. The corrosion testing is conducted on the fabricated composites as per ASTM standard B117-14 to identify the micro hardness, flexural strength and corrosion resistance. The Hank's Balanced Salt Solution (HBSS) was used in corrosion setup. One liter of HBSS solution contains NaCl (800 mg/L), KCl (48 mg/L), Na₂HPO₄ (32 mg/L), KH₂PO₄ (20 mg/L), MgSO₄.7H₂O (20 mg/L), CaCl₂ (15 mg/L), glucose (50 mg/L), phenol red (5 mg/L) and NaHCO₃ (10 mg/L) [20]. The micro hardness testing was conducted to identify the microhardness value of the fabricated AZ91D-Ti composites. The microhardness testing was conducted as per ASTM standard with the help of Vickers microhardness tester. The fabricated composites AZ91D-wt.%Ti (x = 0, 4, 8, 12 and 16) was loaded 350 g for the duration of 15 s while conducting Vickers micro hardness test. The micro hardness test condition was selected based on literature. The ASTM for microhardness was ASTM E384.

The flexural testing was conducted on the fabricated composites as per ASTM standard to identify the flexural strength. The mass loss was determined by determining the mass of the composites before and after the 21 days immersion in HBSS solution. The better combination of AZ91D-Ti composites was further subjected to microstructure analysis to identify the uniform distribution of Ti reinforcement in AZ91D magnesium alloy. The specimen was polished with the help of 600,800 and 100 grit sheets [14]. The roughness average value of polished specimen was 1 µm. The HF acid solution was used to study the microstructure. The microstructure study was done at different thickness of the better combination of fabricated composites to confirm the density of presence of reinforcement in matrix material.

Optimization

A computerized numerically controlled (CNC) milling machine (Tool craft BR3535 NP) was chosen for optimization. The tool craft BR3535 NP has the following specifications and were the work table size of 600 x 400 mm, table movement of longitudinal 450 mm, cross movement of 300 mm, distance from spindle to table 200-450 mm, maximum load capacity of 300 kg, spindle speed of 50000 rpm and machine weight of 1800 kg. The AZ91D-12wt.%Ti was chosen as work piece material and it was subjected to surface grinding to achieve proper flatness before the milling operations. The 1 µm surface roughness was achieved after surface grinding operation. The micro-milling machining employs a smaller sized two-flute flat end mill cutter having a diameter of 500 µm (made by Craft Tool, CT MM C/T 2021-005). The CT MM C/T 2021-005 has the 500 µm diameter with 2 flutes, 4 mm shank and 0.6 mm flute length. The end mill has hardness value of 60 HRC. The tool is made of Wc-Co with 300 helix angle. The optimization was done on the fabricated AZ91D-12wt.%Ti composite with the help of TOPSIS [21]. TOPSIS optimization was used for equating multiple response variables into a single optimal response. The following steps were followed for optimizing of micro machining process parameters by employing TOPSIS technique [22].

Step 1: Formation of normalized matrix from the below equation

$$r_{pm} = \frac{k_{pm}}{\sqrt{\sum_{p=1}^n k_{pm}^2}} \quad m = 1, 2, n \quad (1)$$

where s_{pm} is the performance of p^{th} alternative in relation to the m^{th} attribute.

Step 2: Compute weighted normalized matrix

The weight of each attribute considered was given by w_m ($m = 1, 2, \dots, n$). The weighted normalized decision matrix $U = [u_{pm}]$ can be obtained by

$$U = w_m r_{pm}$$

Step 3: Computation of ideal best and worst value

The optimal positive and negative solutions have been computed from the following expressions:

$$U^+ = \{(\sum_p^{\max} u_{pm} | m \in M), (\sum_p^{\min} | m \in M | p = 1, 2, \dots, m)\} \\ = \{u_1^+, u_2^+, u_3^+ \dots \dots \dots, u_n^+\} \quad (2)$$

$$U^- = \{(\sum_p^{\min} u_{pm} | m \in M), (\sum_p^{\max} | m \in M | p = 1, 2, \dots, m)\} \\ = \{u_1^-, u_2^-, u_3^- \dots \dots \dots, u_n^-\} \quad (3)$$

Step 4: Computing the Euclidean distance (ED) from the ideal worst and ideal best

The "ideal" solution and is given by:

$$s_p^+ = \sqrt{\sum_{m=1}^n (u_{pm} - u_m^+)^2}, \quad p = 1, 2, \dots, m \quad (4)$$

Segregation of variation from "negative-ideal" solution is expressed as:

$$s_p^- = \sqrt{\sum_{m=1}^n (u_{pm} - u_m^-)^2}, \quad p = 1, 2, \dots, m \quad (5)$$

Step 5: Computing performance score

Closeness to the distinct substitute to the optimal positive ideal solution is computed from the following expression:

$$P_i = \frac{s_p^-}{s_p^+ + s_p^-} \quad p = 1, 2, \dots, m \quad (6)$$

Step 6: Ranking

The most and least preferred alternative solutions were identified by distinctly arranging the P_i value in a descending order.

The L9 orthogonal array was selected for this optimization because of its higher prediction ability. The L9 orthogonal array (Taguchi design) was selected for optimization on micro milling process parameters of better combination of fabricated composites. The input parameters selected for optimization were cutting rate (CR), feed rate per tooth (FT), axial depth of cut (DOC) and tool type (TT) and response parameters are Feed force (Fx), normal force (Fy) tool wear rate

(TWR), milling burr height (Buh) and surface roughness (Ra). The surface roughness was measured by using Mitutoyo Surf Test 301 profilometer. The piezo-electric dynamometer along with charge amplifier (Kistler, models 9265C2 and 5010) with an accuracy range of ± 0.2 N was used to find the cutting force. Tool wear and Burr height were measured using a scanning electron microscope (Philips XL30). The input parameters with their levels were cutting rate ((A) 60, 12, 180 m/min), feed rate per tooth ((B) 0.5, 1, 1.5 μm), axial depth of cut ((C) 0.05, 0.15, 0.25) and tool condition ((D) uncoated (A), TiN coated (B), TiB₂ coated (C)). The Taguchi L9 orthogonal array with input and response parameters is shown in Table 1.

Table 1. Input and response parameters in L9 orthogonal array.

EX. No.	A	B	C	D	F _x (N)	F _y (N)	TW (μm)	SR (μm)	Buh (μm)
1	40000	0.5	0.05	A	2.02	1.38	16.89	0.24	48.32
2	40000	1	0.15	B	2.32	1.53	24.72	0.38	39.68
3	40000	1.5	0.25	C	2.71	1.69	30.43	0.48	26.21
4	60000	0.5	0.15	C	2.31	1.75	12.46	0.23	32.56
5	60000	1	0.25	A	2.72	2.16	36.08	0.49	30.27
6	60000	1.5	0.05	B	3.34	2.19	14.17	0.31	20.03
7	80000	0.5	0.25	B	2.79	2.03	27.31	0.27	22.39
8	80000	1	0.05	C	3.68	2.33	32.65	0.31	32.65
9	80000	1.5	0.15	A	4.24	2.48	46.89	0.63	29.81

RESULTS AND DISCUSSION

EDAX testing

The composition of AZ91D matrix material is Si (0.034), Cu (0.002), Ni (0.001), Fe (0.002), Mn (0.03), Pb (0.001), Zn (0.775), Al (8.40), Sn (0.002) and Mg (remaining %). The composition of AZ91D-wt. % Ti (x = 0, 4, 8, 12 and 16) is shown in Table 2. The titanium powder is in the conical shape and it is better to bond with matrix material. The AZ91D magnesium alloy is matrix and Ti is reinforcement material.

Table 2. Composition of AZ91D-Ti composites.

S.No	Composition	Series	Element wt.%				
			Mg	Al	Zn	Mn	Ti
1	AZ91D	K Series	89.84	9.2	0.7	0.17	-
2	AZ91D/4wt.%Ti	K Series	88	7	0.8	0.3	3.9
3	AZ91D/8wt.%Ti	K Series	83	8	0.8	0.6	7.6
4	AZ91D/12wt.%Ti	K Series	78	9	0.7	0.2	12.1
5	AZ91D/16wt.%Ti	K Series	74	8.8	0.9	0.5	15.8

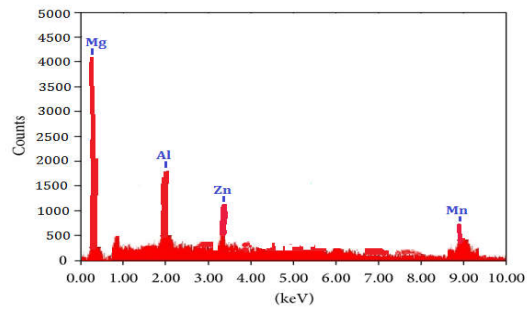


Figure 2a. AZ91D.

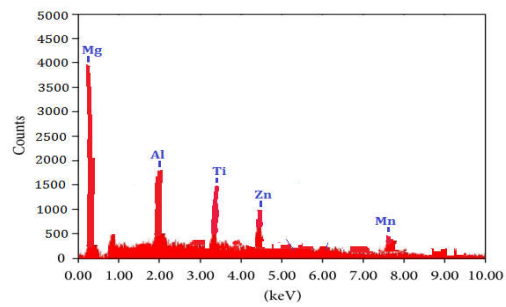


Figure 2b. AZ91D/4wt.%Ti.

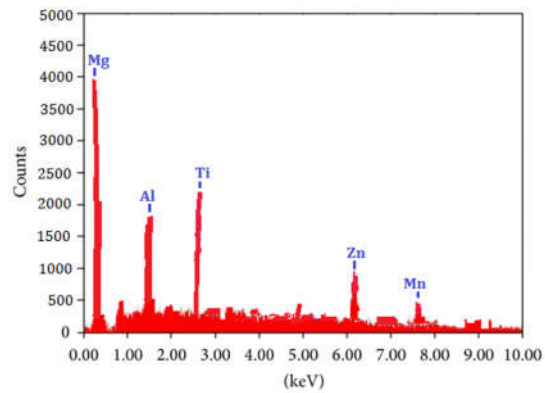


Figure 2c. AZ91D/8wt.%Ti.

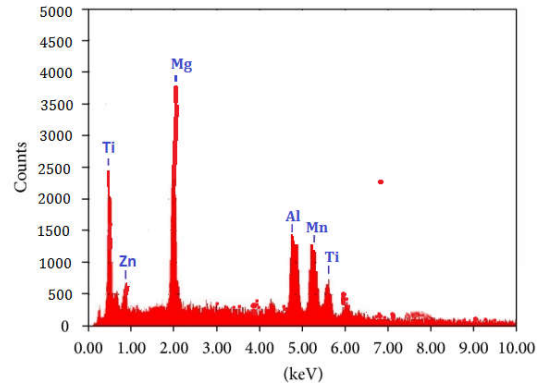


Figure 2.d. AZ91D/12wt.%Ti.

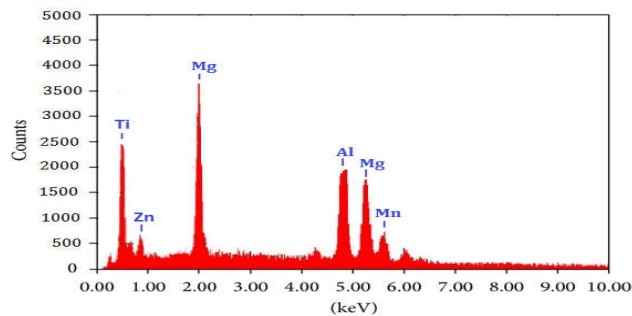


Figure 1e. AZ91D/16wt.%Ti.

The EDAX test results for AZ91D-wt. %Ti ($x = 0, 4, 8, 12$ and 16) composites are shown in Table 2 and Figure 1 (a-e). The EDAX test results confirm that weight percentage of AZ91D and Ti in every fabricated composite is equal to designed composites combination. The AZ91D-12wt. % Ti is the best sample because of its uniform distribution of Ti in matrix material. The wt.% percentage of all elements of fabricated composites are presented in Table 2.

Mechanical, chemical and metallurgical property testing

The fabricated magnesium AZ91D-wt.%Ti ($x = 0, 4, 8, 12$ and 16) composites are subjected to Vickers microhardness test and flexural test under the condition of NaCl based spray. The Vickers microhardness test is conducted on all fabricated composites to identify the microhardness of the produced composites. Three trials are used to find the average microhardness of the produced composites. The micro hardness test and flexural test results are shown in Table 3. The microhardness of each fabricated composites are compared with each other. The microhardness is increased by the addition of titanium reinforcement into AZ91D matrix material. The microhardness is increased up to 12wt. % of Ti addition into magnesium matrix material and decreased by 16wt.% of Ti addition. The high 12wt.% of Ti addition and uniform distribution of 12wt.% Ti in AZ91D matrix material increases micro hardness [23]. The magnesium matrix material is well bonded with titanium reinforcement material. So the high bonding strength increases the microhardness of the fabricated composites. The magnesium is a well suited bonding

agent for the titanium reinforcement grains [24]. The over accumulation of Ti reinforcement particles decrease the bonding strength of the produced composites. The decreasing of bonding strength decreases the micro hardness of the produced composite material and decreased by 16wt.% of Ti addition. The addition of titanium increases the micro hardness because of its high hardness property of titanium in AZ91D/12wt.%Ti composite. The microhardness of AZ91D/16wt.%Ti decreases due to over accumulation of Ti. The micro hardness decreases because of the easy dislocation of matrix and reinforcement material. The dislocation of material is due to the lower bonding strength. The AZ91D-12wt.%Ti composite exhibits higher Vickers microhardness than other fabricated composites.

Table 3. Comparison of Vickers microhardness and Flexural strength of AZ91D/Ti composites.

S. No.	Material	Before corrosion test (NaCl based spray)		After corrosion test (NaCl based spray)	
		Microhardness	Flexural strength (MPa)	Microhardness	Flexural strength (MPa)
1	AZ91D	60	438	58	435
2	AZ91D/4wt.%Ti	78	452	75	448
3	AZ91D/8wt.%Ti	92	475	89	471
4	AZ91D/12wt.%Ti	121	493	120	490
5	AZ91D/16wt.%Ti	116	482	114	479

The flexural strength of the AZ91D/wt.%Ti ($x = 0, 4, 8, 12$ and 16) composites are shown in Table 3. The flexural strength of the composite is increased by the addition of titanium into AZ91D matrix composites. The titanium reinforcement is acted as a load transferring element to matrix material and it prevents the commencement of cracking. The increase of flexural strength is due to fine particle size of titanium reinforcement particles [25, 26]. The high 12wt.% of Ti addition and uniform distribution of 12wt.% Ti in AZ91D matrix material increases the flexural strength. The over accumulation of titanium decreases the microhardness, flexural Strength of AZ91D/16wt.%Ti and it is reduced than AZ91D/12wt.%Ti composite.

Table 4. Comparison of mass loss of AZ91D-wt.%Ti composites.

S. No.	Material	Mass loss (g) 21 days immersion
1	AZ91D	0.089
2	AZ91D/4wt.%Ti	0.081
3	AZ91D/8wt.%Ti	0.075
4	AZ91D/12wt.%Ti	0.059
5	AZ91D/16wt.%Ti	0.068

The fabricated AZ91D based composites is subjected to corrosion test. The fabricated composites are immersed in Hank's Balanced Salt Solution for 21 days. The corrosion resistance of AZ91D based composites is shown in Table 4. The addition of titanium into AZ91D matrix material increases the corrosion resistance of produced composites. The high corrosion resistance is achieved by the addition of 12wt. % titanium reinforcement into AZ91D matrix material. The titanium reinforcement is prevented the degradation of Mg during corrosion test. The Ti corrosion resistance property also contributes the enhancement of corrosion resistance of AZ91D based composites [27]. The 16wt.% of Ti addition decreases the corrosion resistance of fabricated composites is due to increased porosity and decreased bonding strength. From the above mechanical and chemical property testing of AZ91D-wt. %Ti ($x = 0, 4, 8, 12$ and 16) composites, it can conclude that AZ91D-12wt.%Ti composite exhibits better behavior. So AZ91D-12wt.%Ti

composite is selected for further investigation. The bonding strength of AZ91D/12wt.%Ti composite is higher than the AZ91D/16wt.%Ti composite and it is mainly influence the mass loss of the composite. The over accumulation of Ti in AZ91D/16wt.%Ti composite decreases the bending strength.

The microstructure of AZ91D/12wt.%Ti composite is studied with the help of scanning electron microscope. The SEM image of AZ91D/12wt.%Ti composite confirms the dispersion of titanium reinforcement in AZ91D matrix material and it is shown in Figure 2.

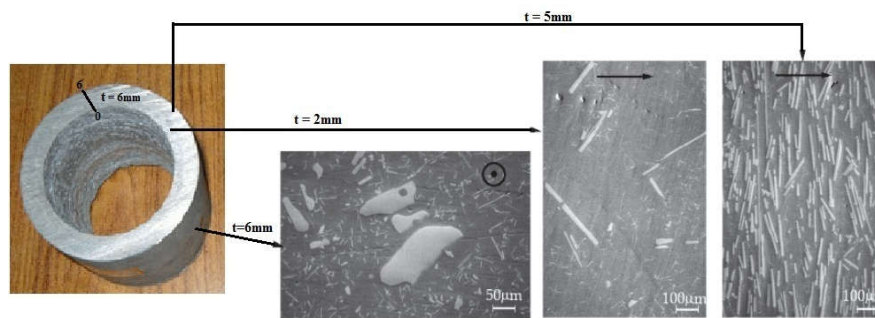


Figure 2. Microstructure of AZ91D/12wt.%Ti composites (50 µm and 100 µm).

The SEM images of AZ91D/12wt.%Ti composite represents the different densities of Ti reinforcement dispersion in matrix material. The different densities are achieved due to the centrifugal force of casting process. The unfurled tubular sections have inner and outer zones respectively; the outer zones usually have higher reinforcement concentration owing to centrifugal forces involved in the fabrication [15]. The side, where the outer zones would exist is chosen for the experimental trials on all the samples. This side is relatively harder and denser than the side that lays in the inner zone direction.

Optimization

The optimization is done on the micro machining process parameters of AZ91D/12wt. %Ti composite by using TOPSIS. The TOPSIS is used for converting multi objective into single objective. The best optimal parameters are determined based on the identified Closeness Coefficient values. The F_x , F_y , TWR, BH and Ra are in the type of 'lower the better'. The Closeness Coefficient is determined with the help of defined equations (1-5). The highest Closeness Coefficient value represents experimental and ideal values are similar. The parameter which is in the closest proximity to the ideal solution is considered the most significant process variable and the ranking is given in that order. From Table 5 it can be seen that the trial run #4 has the closest proximity to the ideal solution and hence ranked #1 followed by trials 6 and 1 that are ranked 2 and 3 respectively. The preferential order-based value determines the optimal settings for the experimentation and is given as $A_2B_1C_2D_3$.

The mean Table 6 reveals that optimum parameters are 120 m/min cutting rate, 0.5 µm feed rate per tooth, 0.05 mm axial depth of cut and TiB₂ coated tool condition and it is also shown in Figure 3. From the main effect plot, the least tool wear can be obtained at the least rate of feed of 0.5 µm/tooth. As the rate of feed increases the tool wear also increases and the highest tool wear is noticed for a rate of feed of 1 µm and the tool wear slightly reduces at 1.5 µm/tooth. The depth of cut also plays an essential role in reducing tool wear and it can be seen that the tool wear constantly increases with the depth of cut [28]. The least tool wear is obtained for the least depth

of cut at 0.05 mm. It is evident that the uncoated tool is least efficient while the TiN coated tool has the minimum tool wear.

Table 5. Closeness Coefficients and its rankings.

Exp. No	Separation measures		Relative closeness	Ranking
	S ⁻	S ⁺		
1	0.159991	0.049174	0.764903473	3
2	0.115419	0.07042	0.621070336	5
3	0.088252	0.097073	0.476201962	7
4	0.177662	0.021623	0.891497074	1
5	0.06676	0.11962	0.358195472	8
6	0.165064	0.029879	0.846731039	2
7	0.126241	0.066268	0.655766432	4
8	0.098704	0.09497	0.509638072	6
9	0.033133	0.177045	0.157643401	9

Table 6. Response Table for TOPSIS.

Source	L1	L2	L3	Best optimal	Condition	Max-min	Rank
Cutting rate (A)	0.6207	0.6988	0.4410	0.6988	A2	0.2578	3
Feed rate per tooth (B)	0.7707	0.4963	0.4935	0.7707	B1	0.2772	2
Depth of cut (C)	0.7071	0.5567	0.4967	0.7071	C1	0.2104	4
Tool type (D)	0.4269	0.7079	0.6258	0.7079	D2	0.2810	1

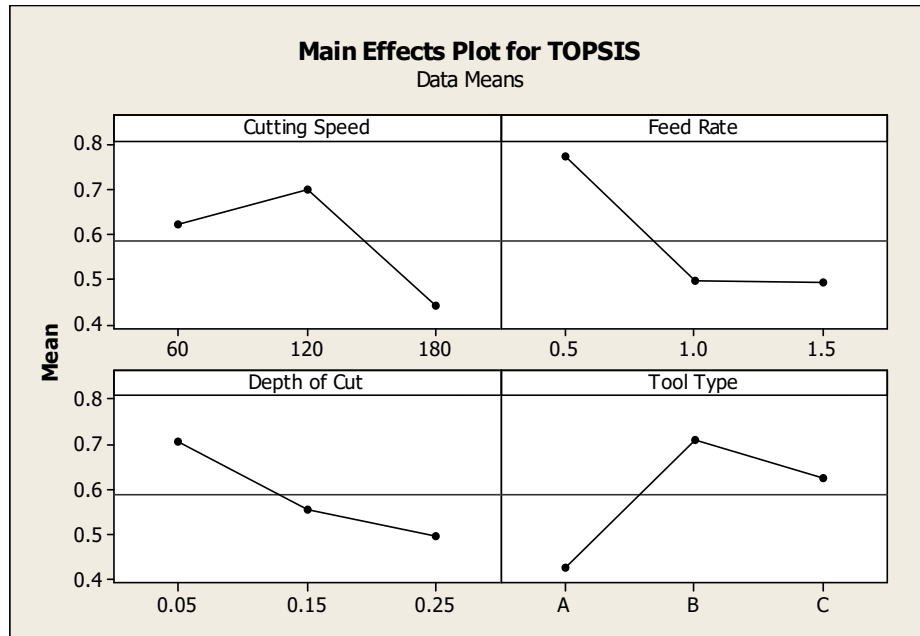


Figure 3. Mean effect plot of CC Vs CS, FT, DOC and TT.

From the Figure 3 it can be observed that the burr height is the smallest when the cutting rate is 120 m/min. Increasing of cutting rate further increases the burr height marginally, but the burr height remains higher at lower cutting rate. The burr height reduces as rate of feed increases and is the lowest for the highest rate of feed of 1.5 $\mu\text{m}/\text{tooth}$. The burr height is higher for the lowest depth of cut and the burr height reduces as the depth of cut increases [9]. The burr height is minimum when the depth of cut is 0.25 mm. The burr height for the uncoated tool is higher when compared with TiB_2 Coated tool. The burr height is lesser for the TiB_2 coated tool. It can be observed from the experimental results that the burr height can be minimized by using medium cutting rate while increasing the depth of cut and rate of feed.

From the Figure 3, the highest cutting speed produces the highest cutting force in x and y directions. F_x and F_y are higher for the cutting rate of 180 m/min and lesser for the lowest cutting rate of 60 m/min. Similarly, the increase in rate of feed also increases the cutting forces the cutting forces of F_x and F_y are higher for 1.5 $\mu\text{m}/\text{tooth}$. The cutting forces of F_x and F_y are minimum for a rate of feed of 0.5 $\mu\text{m}/\text{tooth}$. The depth of cut influences the cutting force along X and Y in a slightly different manner [9]. However, the highest cutting forces are obtained in both the axis (F_x and F_y) for least depth of cut (of 0.5 mm). The uncoated tool tends to have greater cutting forces along both axes. The TiN coated cutting tool exhibited the less cutting force in the X and Y axis. From the Figure 3, the finest surface finish is achieved when the spindle speed is 60000 rpm and the cutting depth is 0.15 mm and the rate of feed is 0.5 $\mu\text{m}/\text{tooth}$. The optimum parameters avoid the formation of buildup edges. The prevention of buildup edges reduces surface roughness.

The ANOVA for TOPSIS is shown in Table 7 and it shows that all input parameters are significant because all P values of all input parameters are less than 0.5 at 95% confidence level. The significance of ANOVA is justified because of square of R almost equal to unity. The contribution percentage is computed by using sequential sum of squares values and it reveals that Tool type has highest influence (30.71%) on CC followed by rate of feed (30.11), depth of cut (17.34) and cutting rate (12.65).

Table 7. ANOVA for TOPSIS.

Source	DF	Seq. SS	Adj SS	Adj MS	F	P	Contribution (%)
Cutting rate	1	0.048443	0.048443	0.048443	1.49237	0.309089	12.65
Rate of feed	1	0.115257	0.115257	0.115257	3.55067	0.156027	30.11
Depth of cut	1	0.066383	0.066383	0.066383	2.04503	0.248063	17.34
Tool type	2	0.125212	0.125212	0.062606	1.92868	0.289366	32.72
Error	3	0.027382	0.097382	0.032461			7.15
Total	8	0.382677					100
R-Sq = 99.58% and R-Sq (adj) = 99.28%							

Confirmation test

The obtained theoretical tests need to be concurred with the outcome of the experimental trials for validating of predictions. The tool wear rate (10.51), feed force (2.06), normal force (1.46), Burr height (23.15), surface roughness (0.22), relative closeness (0.962), relative closeness and percentage improvement in TOPSIS coefficient (7.38). The predicted relative closeness for A2-B1-C1-D2 is 0.918. The TOPSIS outcomes for TWR, F_x , F_y , Buh and SR show the productivity and quality can be improved [29]. The initial settings are considered as A2-B1-C2-D3 while the predicted and experimental settings are A2-B1-C1-D2.

The morphology of machined surface and tool worn surface at optimal process parameters are studied. The material removal is achieved in the form of ribbon because of high amount of matrix

material is removed than its reinforcement. The abrasion wear mechanism is occurred in tool worn surface. The materials are removed by elastic deformation.

CONCLUSIONS

The AZ91D-wt. %Ti ($x = 0, 4, 8, 12$ and 16) composites are fabricated successfully with the help of ex-situ centrifugal casting method. The fabricated AZ91D-Ti composites are subjected to Vickers microhardness test, flexural test and corrosion test to compute the microhardness, flexural strength and corrosion resistance. The AZ91D-12wt.%Ti composite exhibits higher microhardness, flexural strength and corrosion resistance than other produced composites. The addition of Ti into AZ91D matrix material increases microhardness, flexural strength and corrosion resistance up to 12wt.% addition and decreases by the addition of 16wt.% addition. The microstructure AZ91D-12wt.%Ti composite is studied and it reveals that Ti has high dense uniform distribution in matrix material in outer surface AZ91D-12wt.%Ti composite than inner surface because of centrifugal force. The AZ91D-12wt.%Ti composite is subjected to investigation on optimization of micro milling process parameters by using TOPSIS. The following conclusions were made from optimization results. Optimum parameters are 120 m/min cutting rate, 0.5 μm feed rate per tooth, 0.05 mm axial depth of cut and TiB₂ coated tool. Tool type has highest influence (30.71%) on CC followed by rate of feed (30.11%), depth of cut (17.34%) and cutting rate (12.65%). The worn surface of tool at the condition of optimized parameters reveals that abrasion wear mechanism is occurred in tool worn surface.

REFERENCES

1. Bassiouny, S.; Jinghua, J.; Aibin, M.; Dan S. Effect of main parameters on the mechanical and wear behaviour of functionally graded materials by centrifugal casting: A review. *Met. Mater. Int.* **2019**, 25, 1395-1409.
2. Mythili, P.; Janis, L.; Kristine, S.; Dagnija, L.; Alain, L. Biodegradable materials and metallic implants: A review. *J. Funct. Biomater.* **2017**, 15, 148-159.
3. Jia, W.; Jian, K.X.; Chelsea, H.; Dick, H.K.C. Biodegradable magnesium based implants in orthopedics: A general review and perspectives. *Adv. Sci.* **2020**, 7, 1-10.
4. Yuhua, L.; Chao, Y.; Haidong, Z.; Shengguan, Q.; Xiaoqiang, L.; Yuanyuan, L. New developments of Ti-based alloys for biomedical applications. *Mater.* **2014**, 7, 1709-1800.
5. Vaira, V.R.; Padmanaban, R.; Govindaraju, M.; Suganya, P. Mechanical properties and corrosion behaviour of AZ91D-HAP surface composites fabricated by friction stir processing. *Mater. Res. Express.* **2019**, 6, 085401.
6. Rajan, T.P.D.; Pai, B.C. Developments in processing of functionally gradient metals and metal-ceramic composites: A review. *ACTA Metall. Engl.* **2014**, 27, 825-83.
7. Rupesh, K.V.; Digvijay, P.; Manoj, C. A review on fabrication and characteristics of functionally graded aluminum matrix composites fabricated by centrifugal casting method. *Appl. Sci.* **2021**, 3, 227-236.
8. Radha, R.; Sreekanth, D. Insight of magnesium alloys and composites for orthopedic implant applications: A review. *J. Magnes. Alloy.* **2017**, 5, 286-312.
9. Mian, A.J.; Driver, N.; Mativenga, P.T. Micromachining of coarse-grained multi-phase material. *Proc. Inst. Mech. Eng. B: J. Eng.* **2009**, 223, 377-385.

10. Fatih, A.; Ali, E.; Kubilay, A.; Danil, Y.P.; Khaled, G.; Avinash, L.; Muhammad, A. Measurement of micro burr and slot widths through image processing: Comparison of manual and automated measurements in micro-milling. *Sensor*. **2021**, *21*, 4432.
11. Nurettin, S.; Zafer, E.; Said, M.; Aydin, T.; Muammer, K. Review of magnesium-based biomaterials and their applications. *J. Magnes. Alloy*. **2018**, *6*, 23-43.
12. Cardoso, P.; Davim, J.P. Optimization on surface roughness in micromilling. *Mater. Manuf. Process*. **2010**, *25*, 1115-1119.
13. Aatthisugan, I.; Razal, A.; Jebadurai, D. Mechanical and wear behaviour of AZ91D magnesium matrix hybrid composite reinforced with boron carbide and graphite. *J. Magnes. Alloy*. **2017**, *5*, 20-25.
14. Aravindan, S.; Rao, P.V.; Ponappa, K. Evaluation of physical and mechanical properties of AZ91D/SiC composites by two step stir casting process. *J. Magnes. Alloy*. **2015**, *3*, 52-62.
15. Mohamed, G.; Mohamed, S.; Robert, A. Improving the corrosion resistance of AZ91D magnesium alloy through reinforcement with titanium carbides and borides. *J. Magnes. Alloy*. **2015**, *3*, 112-120.
16. Navarro, M.; Michiardi, A.; Castano, O.; Planell, J.A. Biomaterials in orthopaedics. *J. Royal Soc. Interface* **2008**, *5*, 1137-1158.
17. Ashok, R.; Pavendhan, K.; Kumaragurubaran, M. Investigation into tribological behavior of Al7075 and Al7075 based composite. *Trans. Famena* **2020**, *20*, 1-12.
18. Zhiguang, Z.; Duszczuk, J. Magnesium-based composite with improved in vitro surfaces biocompatibility. *J. Mater. Sci*. **2010**, *21*, 3163-3169.
19. Rohatgi, P.K.; Daoud, A.; Schultz, B.F.; Puri, T. Microstructure and mechanical behavior of die casting AZ91D-Fly ash cenosphere composites. *Compos. Part A Appl. Sci*. **2009**, *40*, 883-896.
20. Kirkland, N.T.; Birbilis, N.; Staiger, M.P. Assessing corrosion of biodegradable magnesium implant: A critical reviews of current methodology and their limitation. *Acta Biomater*. **2012**, *8*, 25-936.
21. Arun, K.; Routara, B.C. Multiresponses optimization of process parameter in turning of GFRP using TOPSIS method. *Int. Sch. Res. Notices* **2014**, *4*, 1-10.
22. Mangapathi, R.D.; Vinay, K.K.; Chandra, S.; Singaravel, B. Optimization of EDM process parameters using TOPSIS for machining AISI D2 steel material. *J. Mat. Pr*. **2021**, *46*, 701-706
23. Baraa, H.; Al, K. Study the addition effect of nano and micro titanium on the mechanical properties of PMMA composites. *J. Univ. Babylon Eng. Sci*. **2020**, *28*, 1-8.
24. Umeda, J.; Kawakami, M.; Kondoh, K.; Ayman, E.S.; Imai, H. Microstructural and mechanical properties of Ti particulates reinforced magnesium composite material. *Mater. Chem. Phys*. **2010**, *123*, 649-657.
25. Mohammed, S.; Pugh, M.; Medraj, M. Processing and characterizations of in situ (TiC-TiB₂)/AZ91D magnesium matrix composite. *Adv. Eng. Mater*. **2013**, *15*, 708-717.
26. Mohamad Rodzi, S.N.H.; Zuhailawati, H.; Dhindaw, B.K. Mechanical and degradation behavior of biodegradable magnesium/zinhydroxyapatite with different powder mixing technique. *J. Magnes. Alloy*. **2019**, *7*, 566-576.
27. Nayak, B.B.; Mahapatra, S.S. Multi-responses optimization of WEDM process parameter using the AHP and TOPSIS methods. *Int. J. Theor. App. Res. Mech. Eng*. **2013**, *2*, 109-115.
28. Ramesh, S.; Karunamoorthy, L.; Palanikumar, K. Measurements and analysis of surface roughness in turning of aerospace titanium alloy (GR5). *Measurement* **2012**, *45*, 1266-1276.
29. Kuram, E.; Ozcelik, B. Multi-objectives optimization by using Taguchi based GRA for micro-milling of aluminium 7075 material with ball nose end mill. *Measurement* **2013**, *46*, 1849-1864.